

Connecting coronal 3D electron density from tomographic reconstructions to in-situ measurements from Parker Solar Probe

P. Lamy¹ and J. Wojak²

- (1) Laboratoire Atmosphères Milieux et Observations Spatiales (LATMOS)
- (2) Aix Marseille Université, Institut Fresnel

EGU General Assembly, Vienna 22-28 April 2023

How to obtain the 3D configuration of the corona and its physical parameters at the times of PSP encounters?

→ 3D MHD models

- MAS (Predictive Science Inc.)
- AWSoM (University of Michigan)
- WindPredict-AW (IRAP)

Provide all plasma parameters (N , T , V , B ...) but are not always accurate, see Lamy, Floyd, Mikic, Riley, Solar Phys. 2019 conclusion:

"The MHD models are generally able to match the observed structure and photometry of the corona albeit with various degrees of fidelity for which there is no obvious explanation. However, two limitations emerge, the complexity of coronae of the maximum type and the time lapse between the completion of the magnetograph measurements and the prediction."

→ Solar Rotational Tomography using coronagraphic observations

Provide 3D distribution of the electron density N_e

Comparison MHD - PSP: 2 examples

The following two slides show examples of comparison between MHD calculations and in-situ PSP measurements during E1

- Reville et al. (ApJ Sup Series 246:24, 2020)

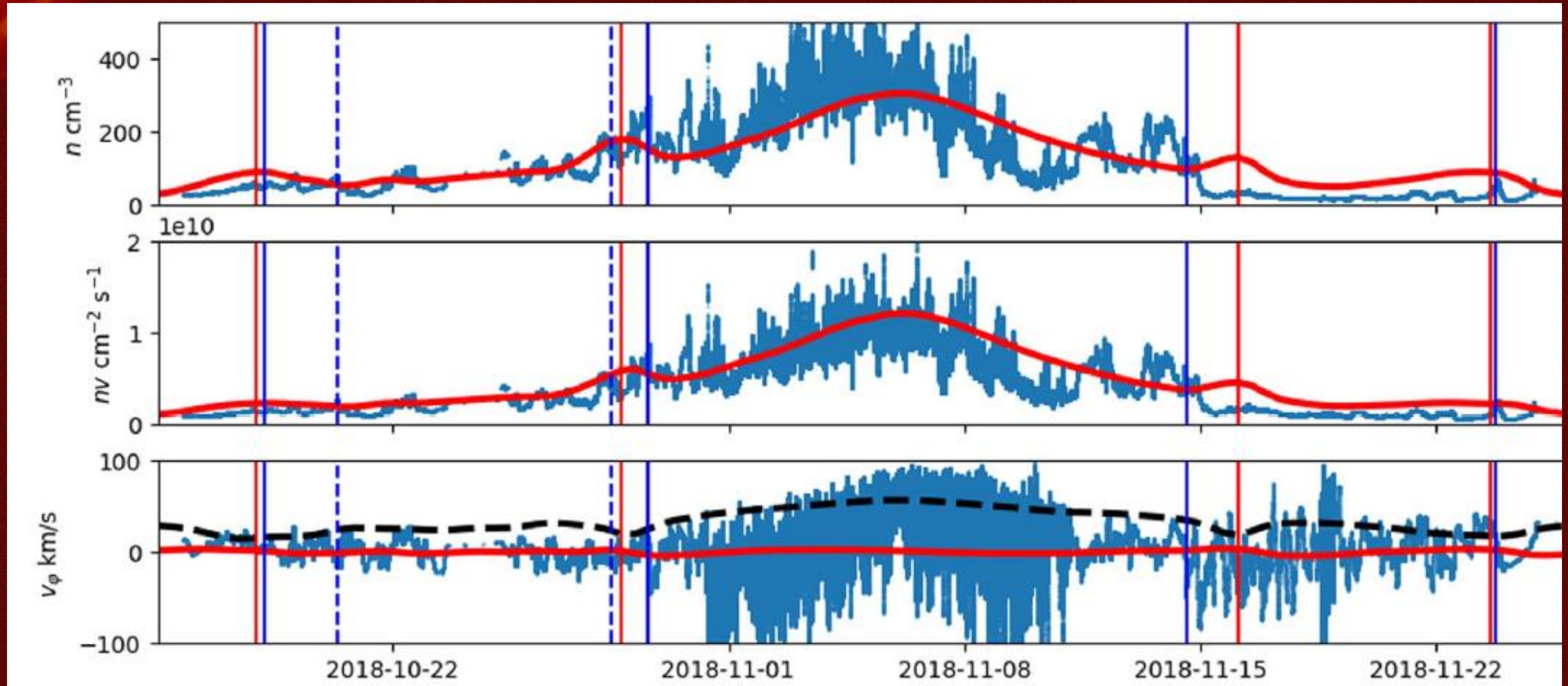
They solved the MHD equations in conservative form for the background and the contribution of the wave energy is accounted for.

- Riley et al. (A&A 650, A19, 2021)

They used three different « MAS » models (Predictive Science Inc.), polytropic, thermodynamic, and = Wave-Turbulence-Driven (WTD)

The agreements range from acceptable to poor. Surprisingly, the WTD solution of Riley et al. is disappointing. Generally, the small-scale variations are not reproduced by the MHD solutions.

E1: Reville et al. 2020



Blue curve: data, red curve: MHD simulation

E1: Riley et al. 2021

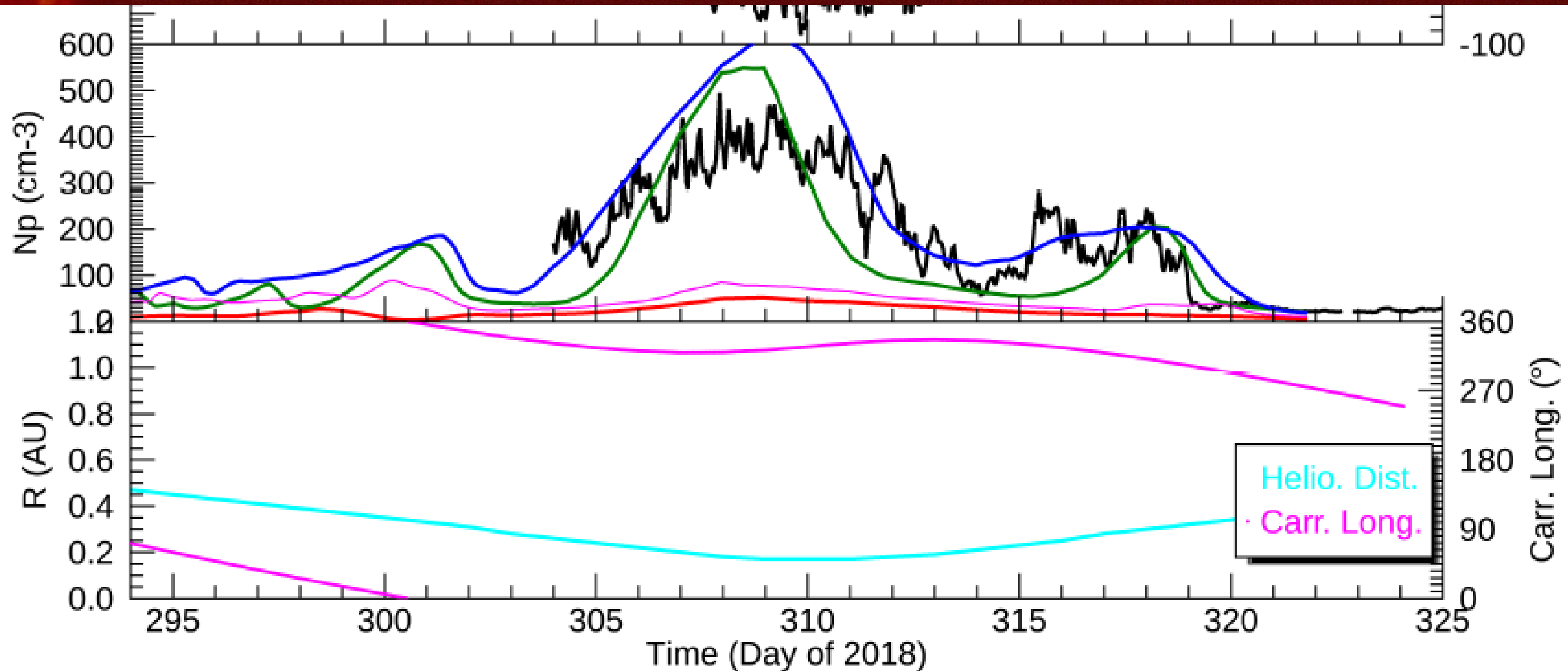


Fig. 3. Comparison of model results with PSP in situ measurements during encounter 1. *From top to bottom:* speed, radial magnetic field, and number density (V_r , B_r , and N_p , respectively) are compared with WTD (red), polytropic (green), and thermodynamic (blue) solutions. Additionally, for P1, the original prediction made by Riley et al. (2019a) is also shown (magenta). Values of B_r , with the exception of the prediction, were multiplied by a factor of three. *Bottom panel:* heliocentric distance (cyan) and Carrington longitude (magenta) are shown as a function of time.



3D Inversion based on static SRT (Solar Rotational Tomography)

- SRT requires continuous observations over half a solar (14 days) to achieve a complete view of the solar corona in the general case of a single vantage point.
- In a first simple approach, the corona is assumed to be static during this time interval.
- Probably valid during minima of solar activity but highly questionable during maxima.
- Initially developed by Altschuler and Perry (1972) and applied to Skylab data by Altschuler (1979).
- Many efforts by different groups using long time series of observations from the SOHO and STEREO missions and also from the Mauna Loa Solar Observatory K-coronameters, see Aschwanden (2011) for a summary until 2011.
- Noteworthy works include: Zidowitz et al. (1996, 1997, 1999), Butala et al. (2005), Frazin et al. (2002, 2005, 2007, 2010), Kramar (2009, 2014, 2016), and Morgan et al. (2009, 2010).
- Tomographic reconstructions using EUVI emissions have also been performed.

3D Inversion based on time-dependent SRT











- First attempt to develop a full time-dependent tomographic reconstruction performed by Butala et al. (2010) who implemented a procedure based on Kalman filters. It left the time-dependent tomography problem under-determined and the solution very reliant on the regularization choices.
- Vibert et al. (2016) achieved a time-dependent tomographic reconstruction by implementing a simpler spatio-temporal regularization. The respective weights of the spatial and temporal regularizations were determined by reconstructing a time-varying model of the corona.
- The procedure was successfully applied to a set of 53 LASCO-C2 pB images from 15 to 29 March 2009.
- Its application to the presently available 25 years [1996-2021] of LASCO-C2 pB images encompassing two complete solar cycles, SC 23 and 24, is almost complete.
- A large part of the resulting Ne "cubes", one every 4 days, is available on a dedicated website: <http://idoc-lasco-c2-archive.ias.u-psud.fr>

LASCO-C2

LEGACY ARCHIVE

Documentation & Data Access

Select a category below to display its content. A link to data access will appear when applicable.

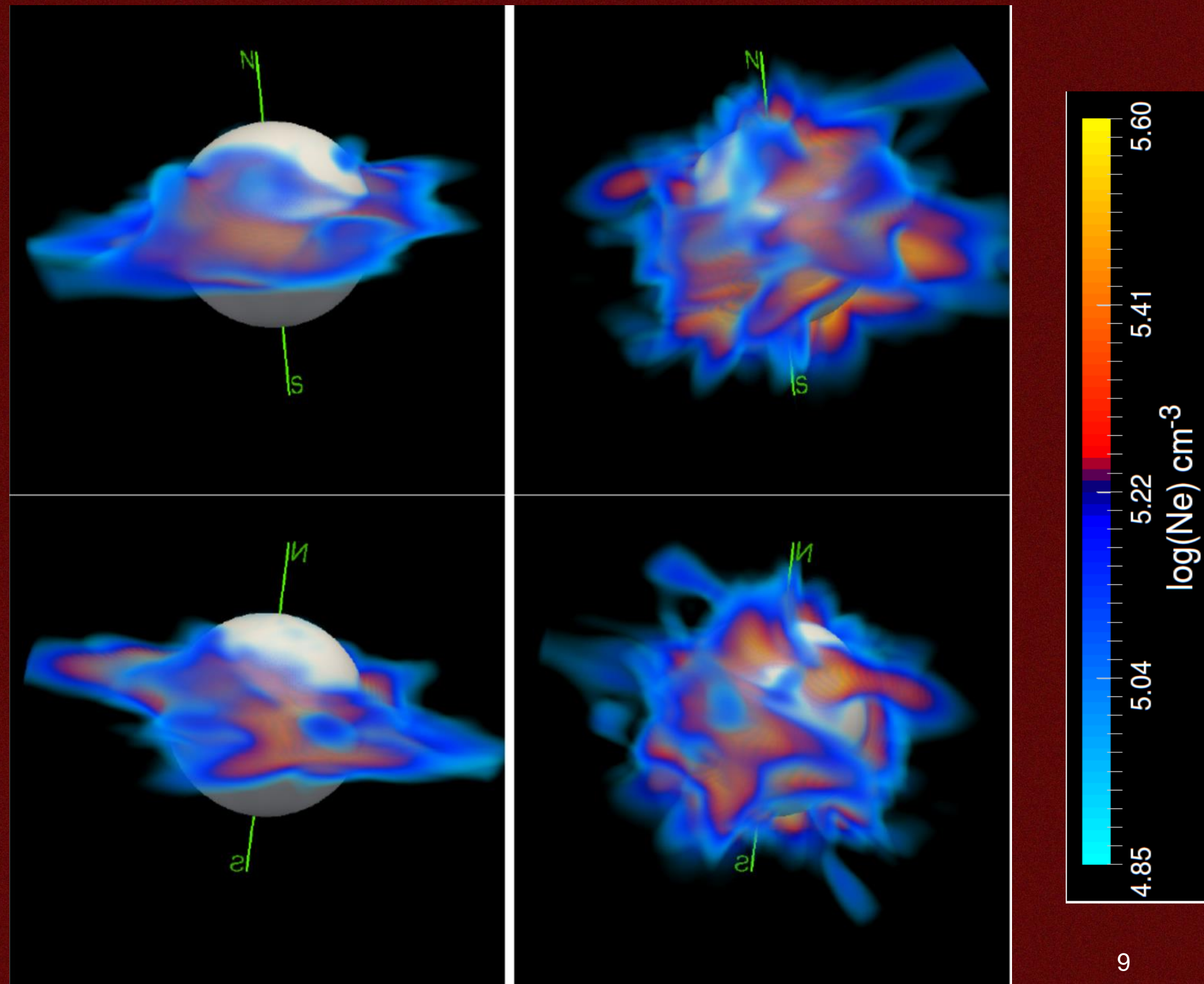
	General Information and Data Policy
	LASCO-C2 Instrument, Operation and Calibration
	LASCO-C2 Data Processing
	LASCO-C2 Scientific Products
	Visualization of Bk data
	ARTEMIS Catalog of CMEs
	ARTEMIS-P Catalog of Polarized CMEs
	3D Electron Density 
	LASCO-C2 Processing Team

Two examples of 3D inversions

Left: CR 1931
Minimum corona

Right: CR 2146
Maximum corona

The white sphere has a radius of 2.5 R_{sun} , the inner limit of the FoV of LASCO-C2



Methodology

- LASCO -C2 pB images accurately corrected and calibrated (Lamy et al. Solar Phys. 2020).
- Time-dependent tomographic reconstruction (Vibert et al. Astr. Computing 2016) performed over a sliding window of 14 days (half a Carrington rotation) with a time interval of 4 days.
- For the present PSP application, the above window is centered at the times of the PSP perihelion.
- The 3D electron density N_e is visualized from six different vantage points.
- The orbit of PSP is projected on a synoptic map of N_e at a heliocentric distance of 5.5 R_{sun} correcting for ballistic solar wind propagation.
- The electron density values at 5.5 R_{sun} are extrapolated to the heliocentric distances of PSP using an inverse square law and are compared with the PSP local measurements.

Ballistic solar wind propagation (Badman et al. 2020)

To accomplish this, we use the Parker spiral (Parker 1958) approximation in which we assume each point along the *PSP* trajectory is threaded by a Parker spiral field line with a curvature determined by the in situ solar wind speed, giving the spiral the following 2D parameterization of longitude and radius (ϕ , r):

$$\phi(r) = \phi_0 - \frac{\Omega_{\odot}}{V_{\text{SW}}}(r - r_0) \quad (1)$$

where ϕ_0 , r_0 are the longitude and radial distance of *PSP* at the time of the V_{SW} measurement. Ω_{\odot} is the solar rotation rate which we calculate from the equatorial rotation period of 24.47 days, assuming the latitudinal offset of *PSP* ($<5^{\circ}$) is small enough to not consider differential rotation.

We take into account the variation of V_{sw} with longitude/time using the *SWEAP* measurements

PSP Encounter 1

P1: 2018-11-06 at 0.166 AU = 35.7 R_{sun}

Supporting references:
 Kasper et al. 2019 ----->
 Bale et al. 2019
 Moncuquet et al. 2020
 Reville et al. 2020
 Riley et al. 2021

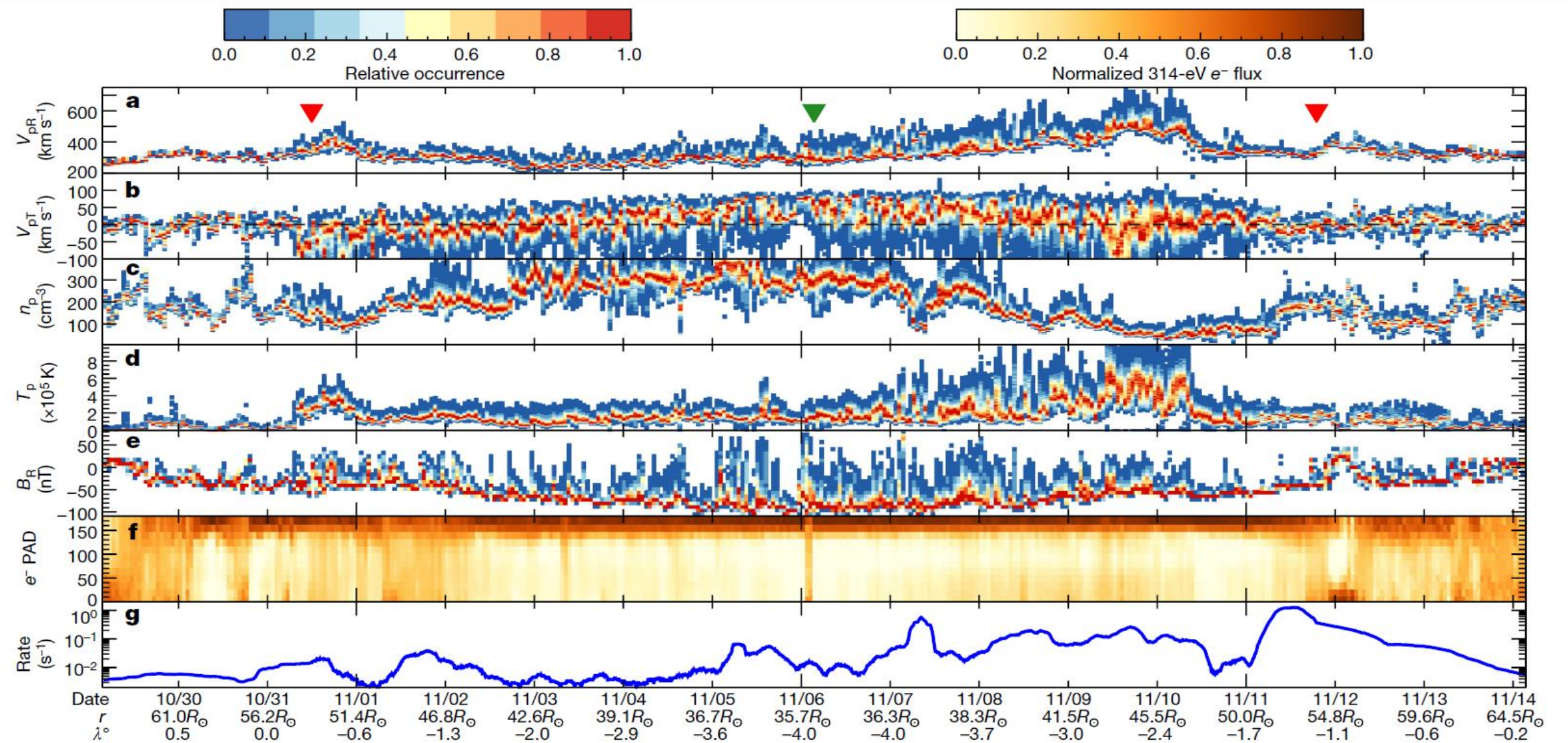
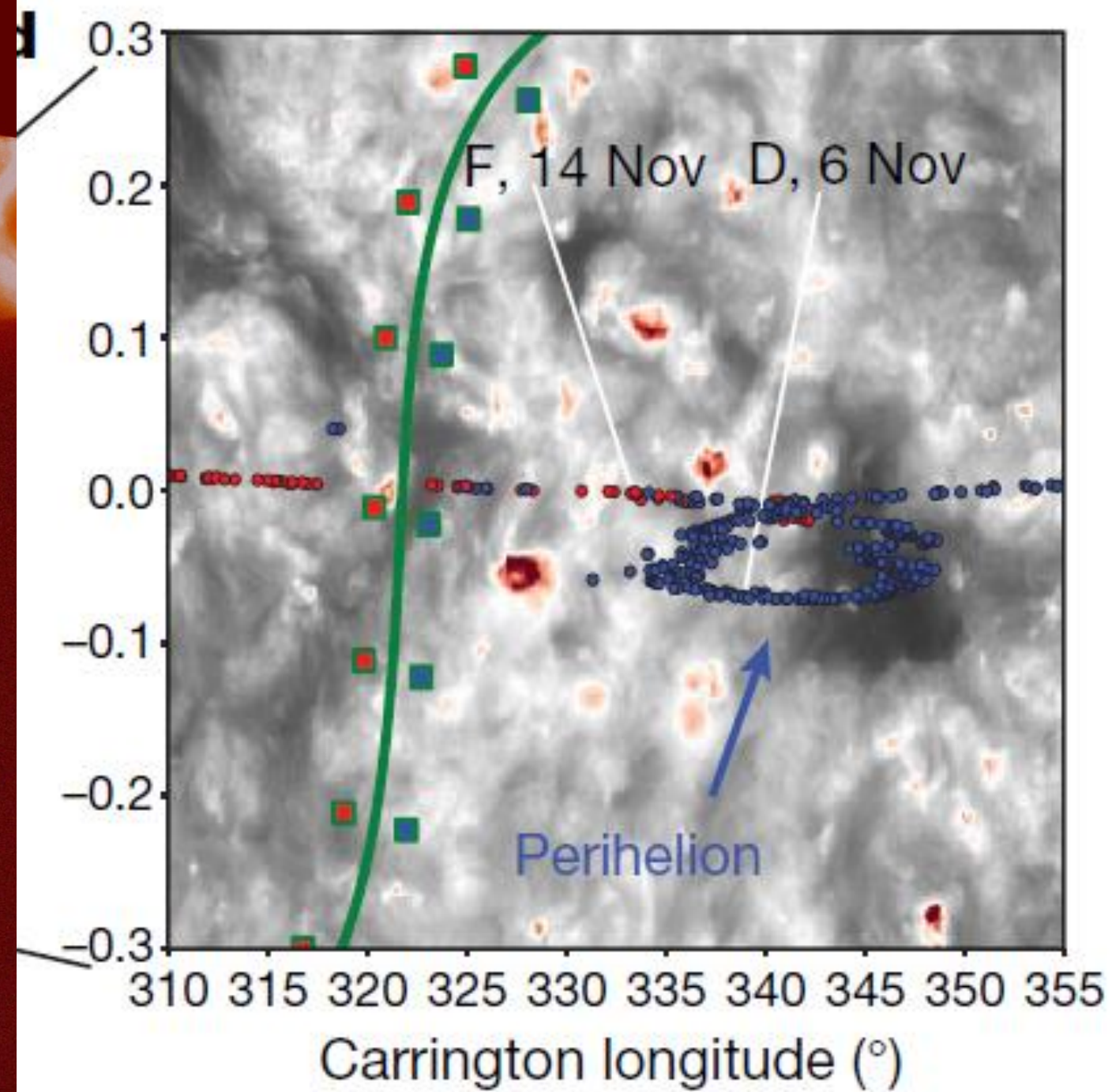


Fig. 1 | Overview of the first encounter of PSP with the Sun. **a**, Relative occurrence rate of the proton radial speed V_{pR} in one-hour intervals. Red triangles show the start and end of the high-rate data collection below $54R_{\odot}$ and the green triangle indicates a perihelion at $35.7R_{\odot}$. **b-f**, The same for V_{pT} in the solar equatorial plane (**b**), the proton number density n_p (**c**), the proton temperature T_p (**d**), the radial component of magnetic field B_R (**e**), the electron pitch-angle distribution (PAD) (**f**) and the 20–200 keV proton rate (**g**). The date (month/day), distance r and latitude λ relative to the solar equator are indicated at daily intervals.



- PIL, $R_{SS} = 2.0R_{\odot}$
- PIL, $R_{SS} = 1.2R_{\odot}$
- (□) Outward (inward) polarity near PIL
- (○) Outward (inward) polarity at spacecraft

↑ Bale et al. 2019

Reville et al. 2019 →

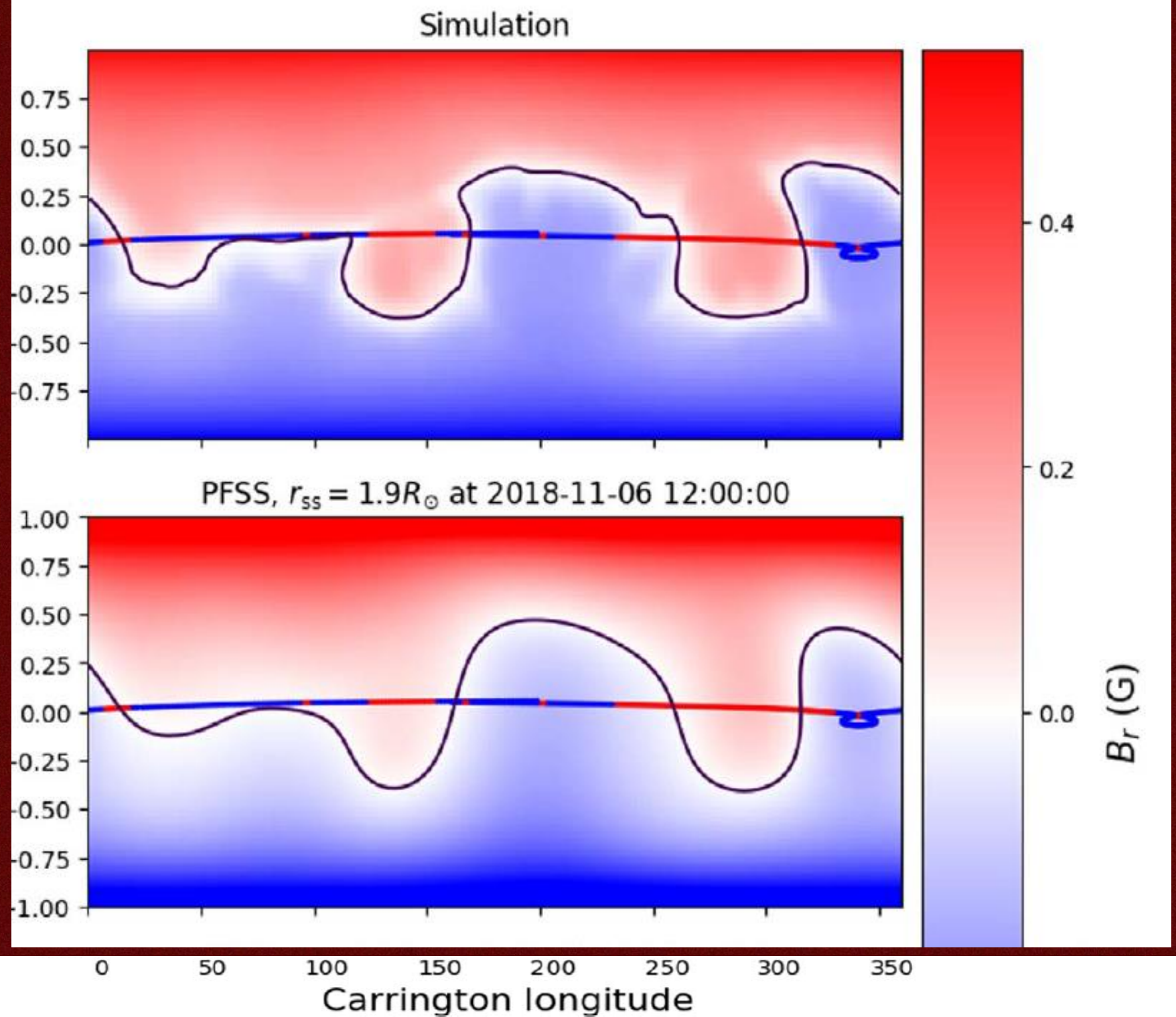
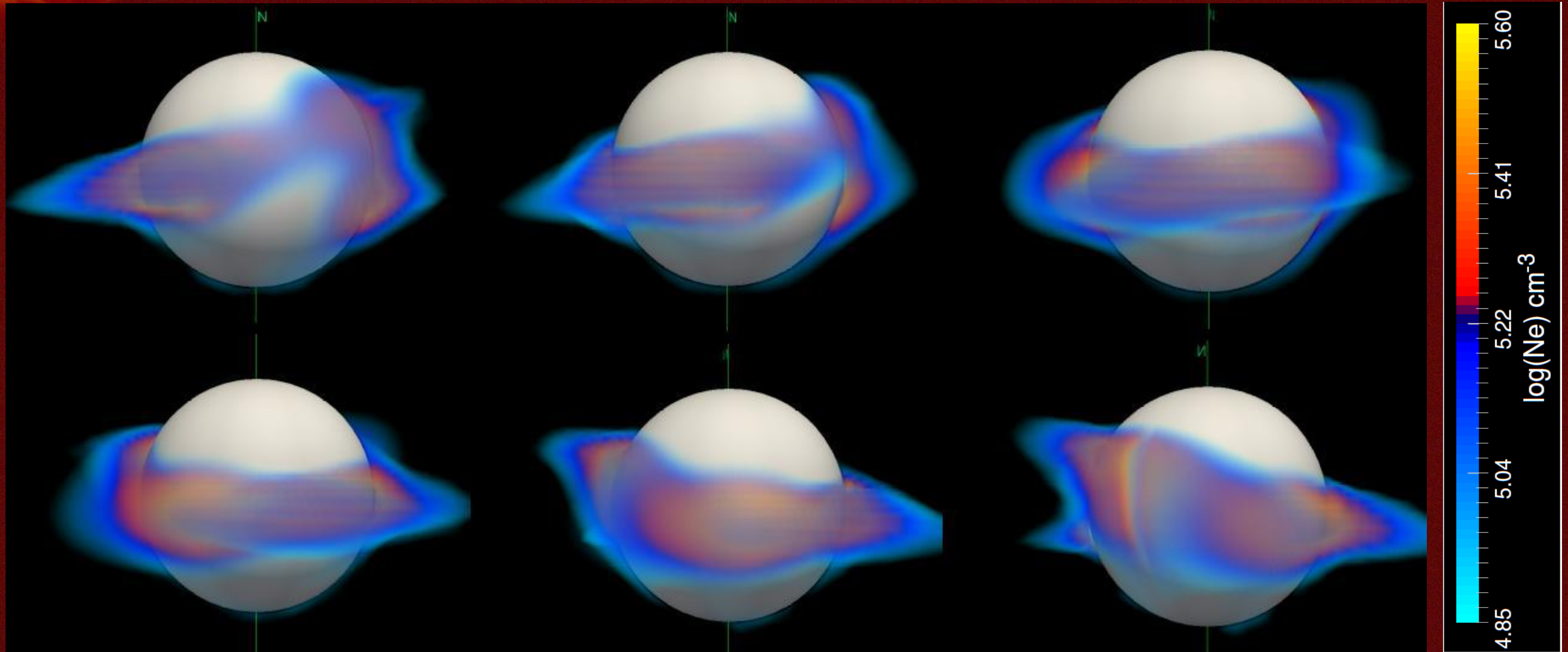


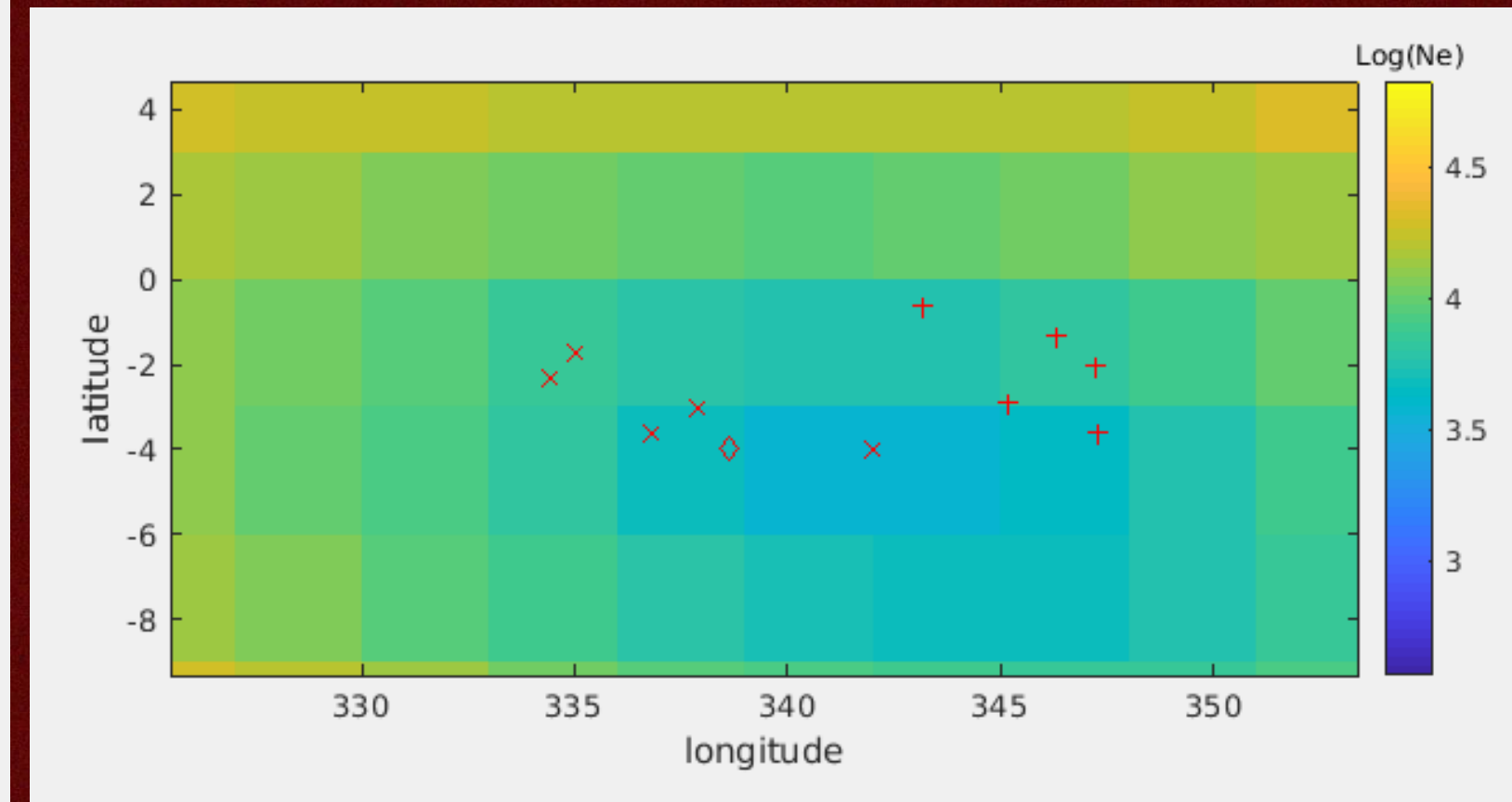
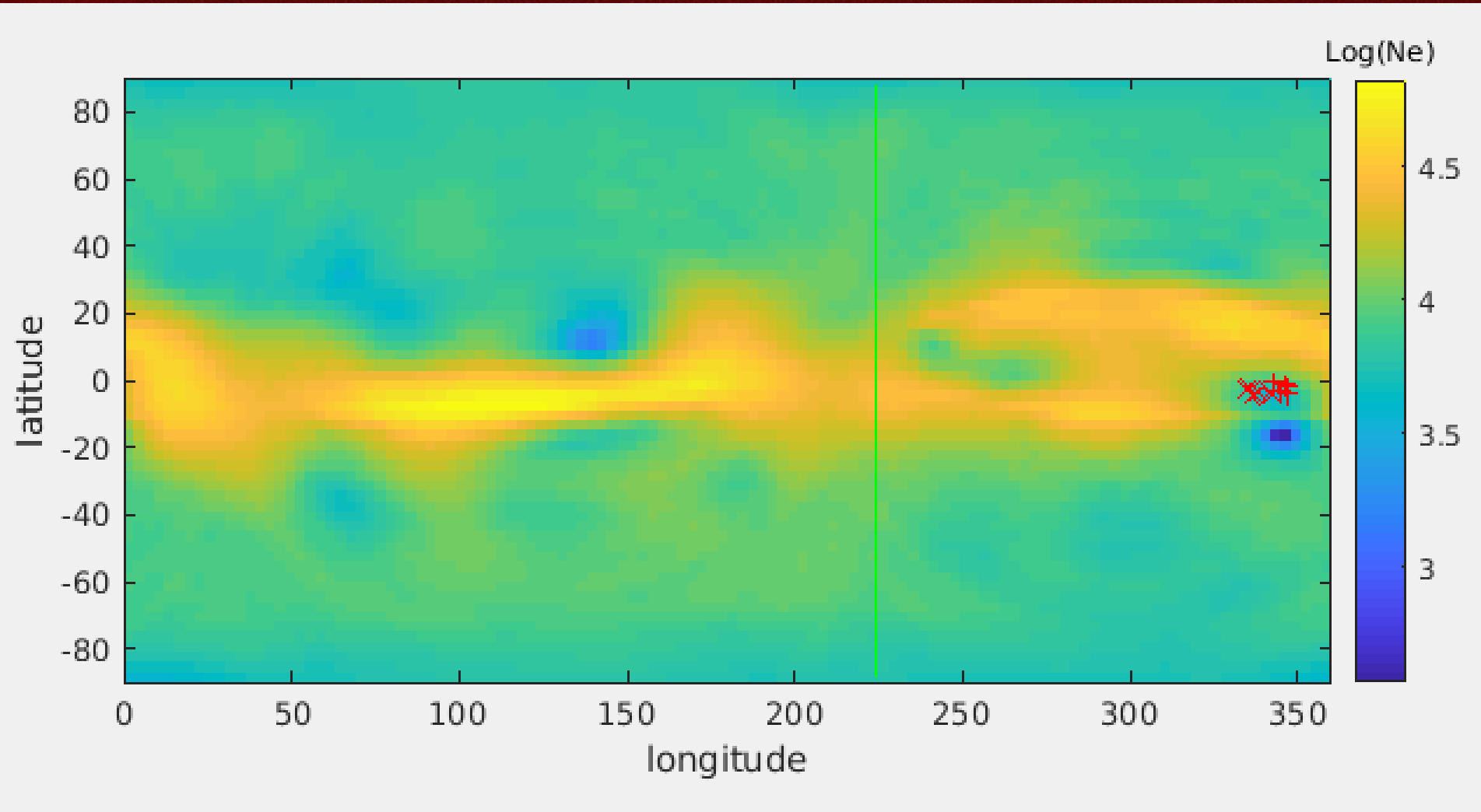
Figure 3. Magnetic field structure at $1.9 R_{\odot}$ in the MHD simulation (upper panel), a PFSS extrapolation using the same magnetic map (middle panel), and another PFSS extrapolation on the October 31 map. The trajectory of the spacecraft between October 15 and November 30 is projected with colors corresponding to the measured polarity. We see that the MHD simulation and the PFSS modeling are close at $1.9 R_{\odot}$ for a given time, and that the earlier map recovers well the polarity change before the perihelion.

Six views of the 3D distribution of the electron density on 2018-11-06 (E1)



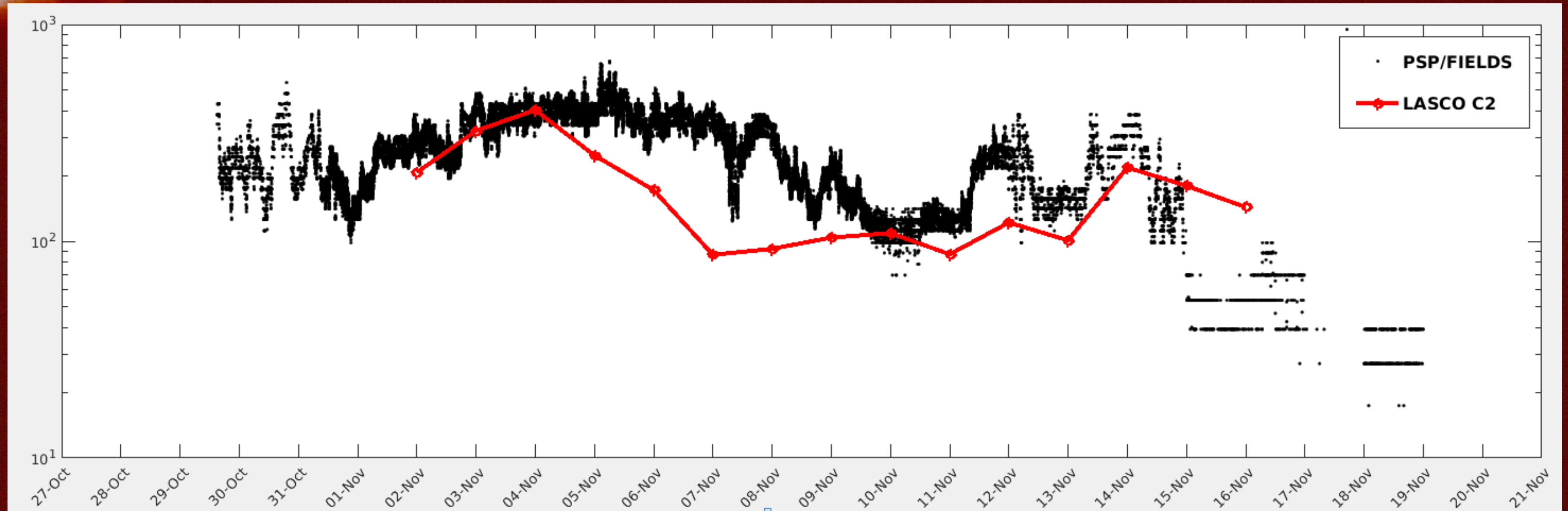
The white sphere has a radius of $2.5 R_{\text{sun}}$

E1: 2018-11-01 to 2018-11-11



Carrington map and zoomed extract of the electron density (cm^{-3}) at 5.5 R_{sun} and the 11 projected locations of PSP over a time interval of ± 5 days (+) centered at perihelion (\diamond).

Profile of the electron density (cm^{-3}) along the orbit of PSP during E1

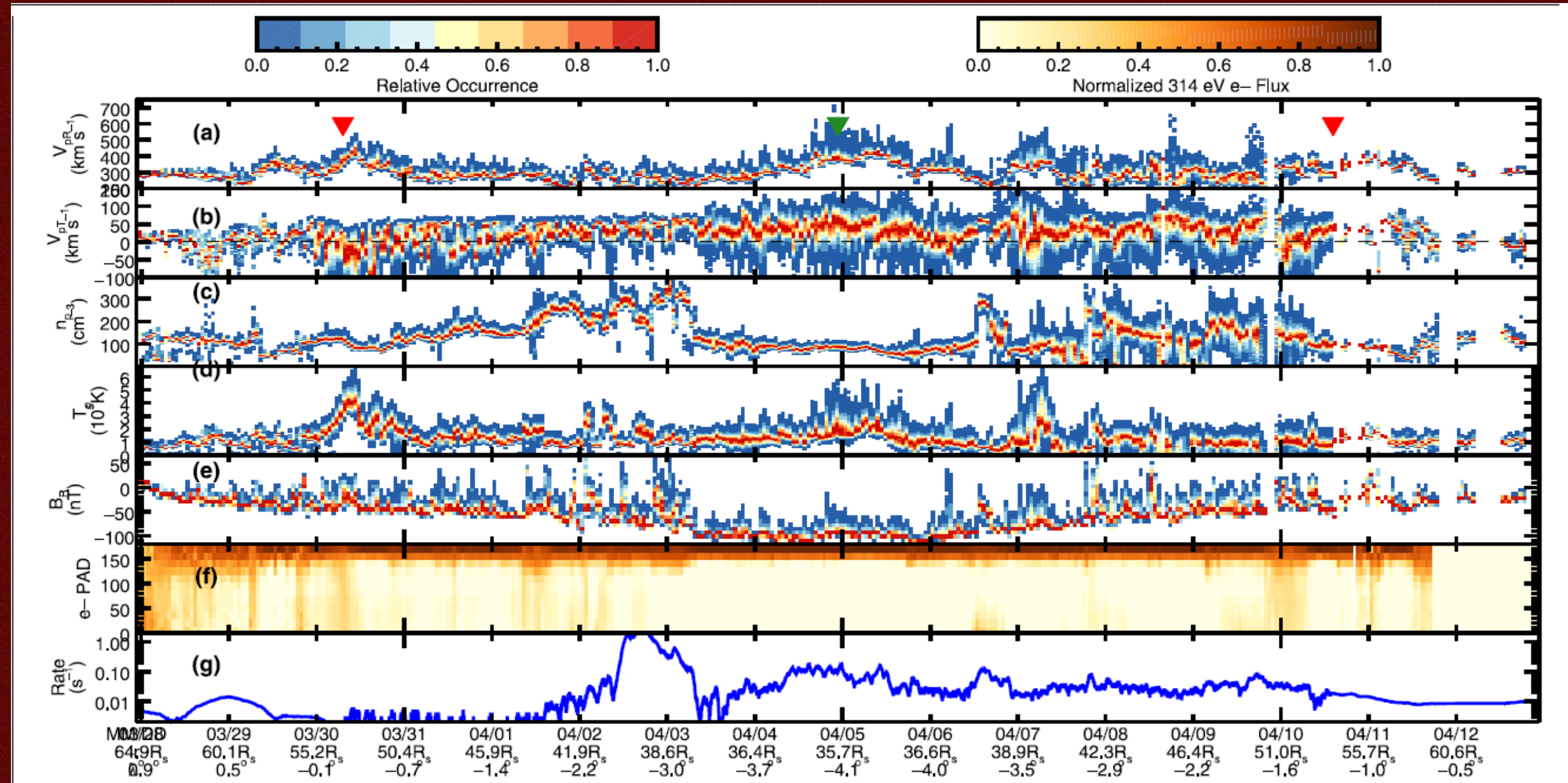


Comparison of the profile from PSP/FIELDS measurements (Moncuquet et al. 2019, black line) with the LASCO-C2 coronal densities at 5.5 R_{sun} extrapolated to the PSP heliocentric distances using an inverse square law. The time interval of ± 5 days is centered on the perihelion date.

PSP Encounter 2

P2: 2019-04-05 at 0.166 AU = 35.7 R_s

Supporting references:
Kasper et al. 2019 ----->
Moncuquet et al. 2020
Riley et al. 2021

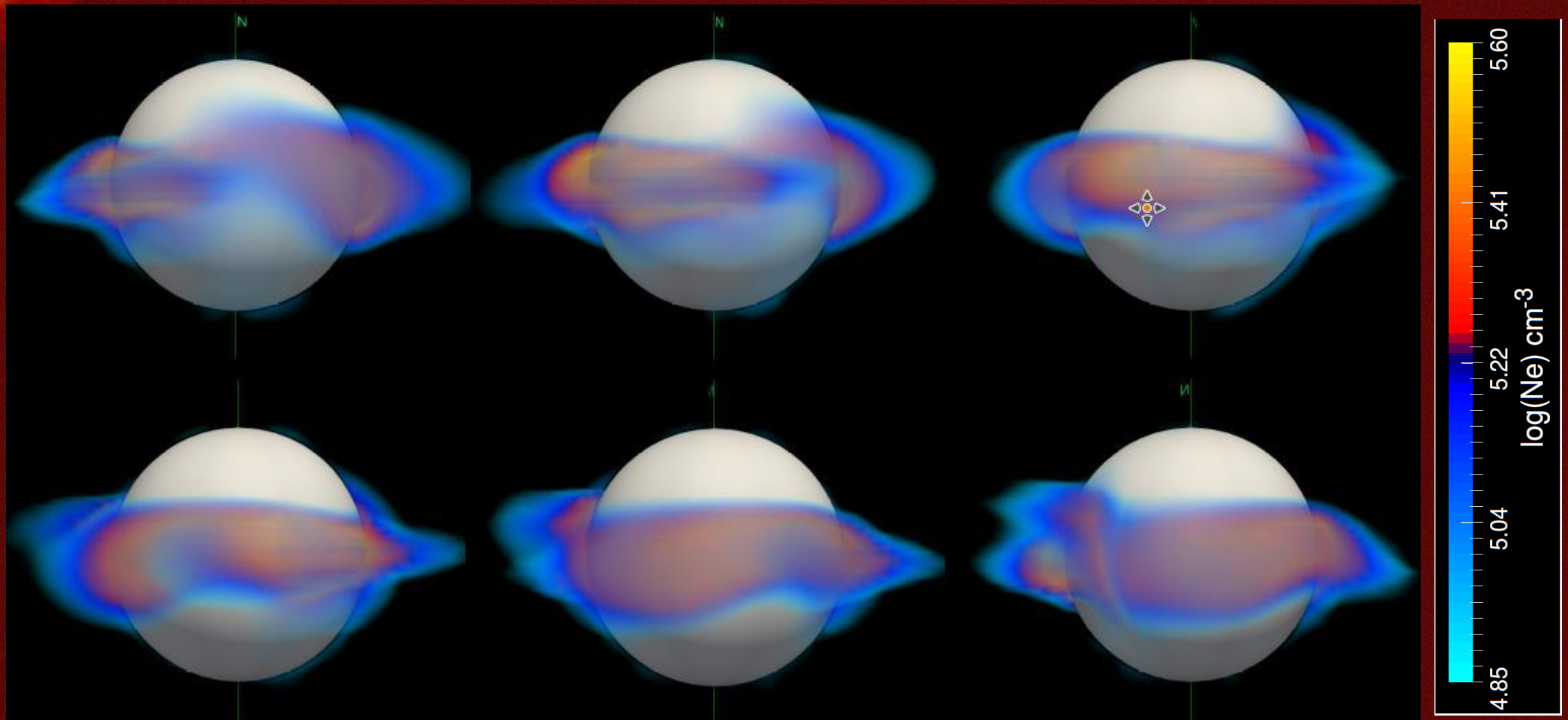


Extended Data Fig. 1 | Overview of the second PSP encounter with the Sun.

The figure is in the same format as Fig. 1. Spikes in the velocity are again seen to be coincident with the magnetic-field reversals, but the jump in the speed is

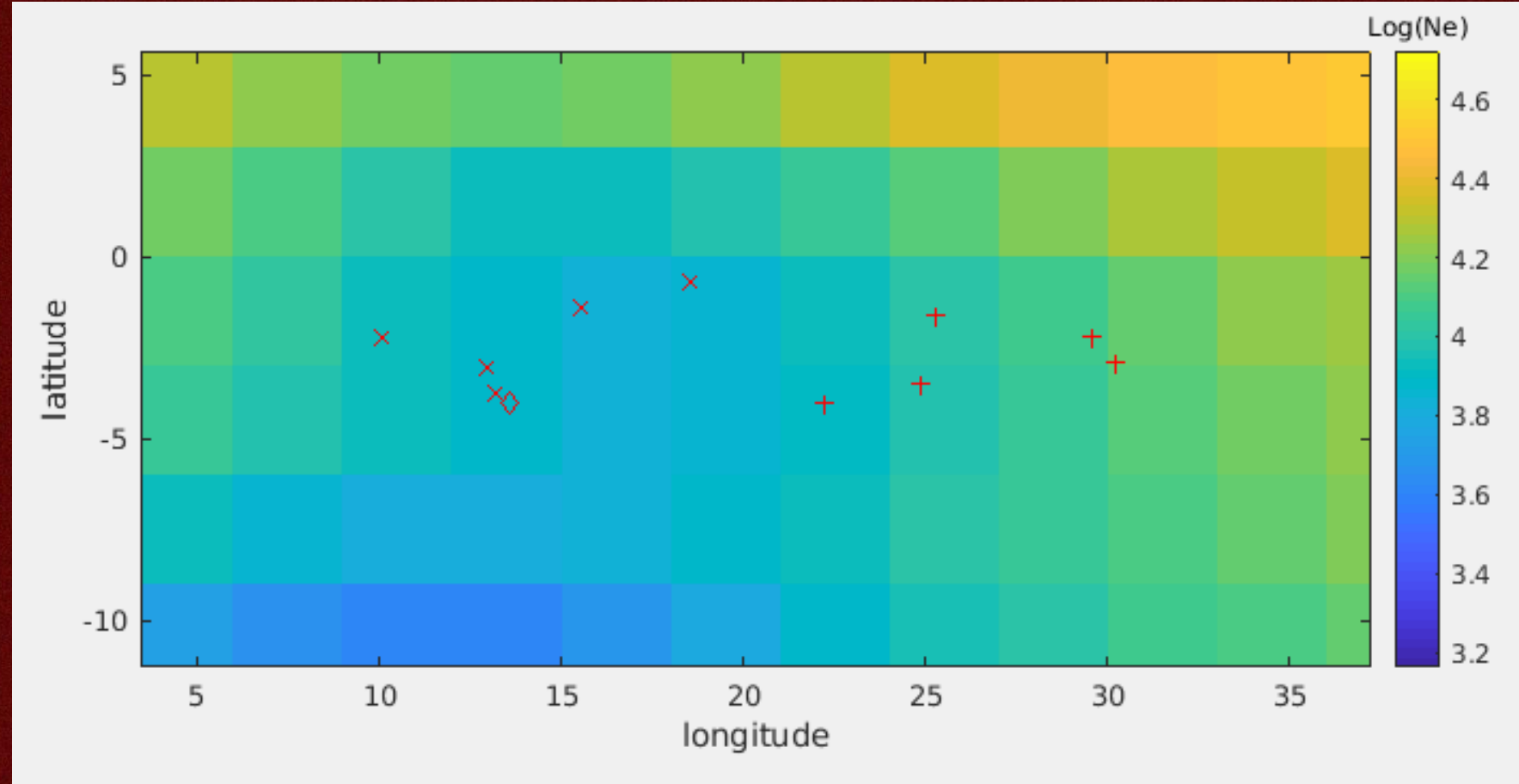
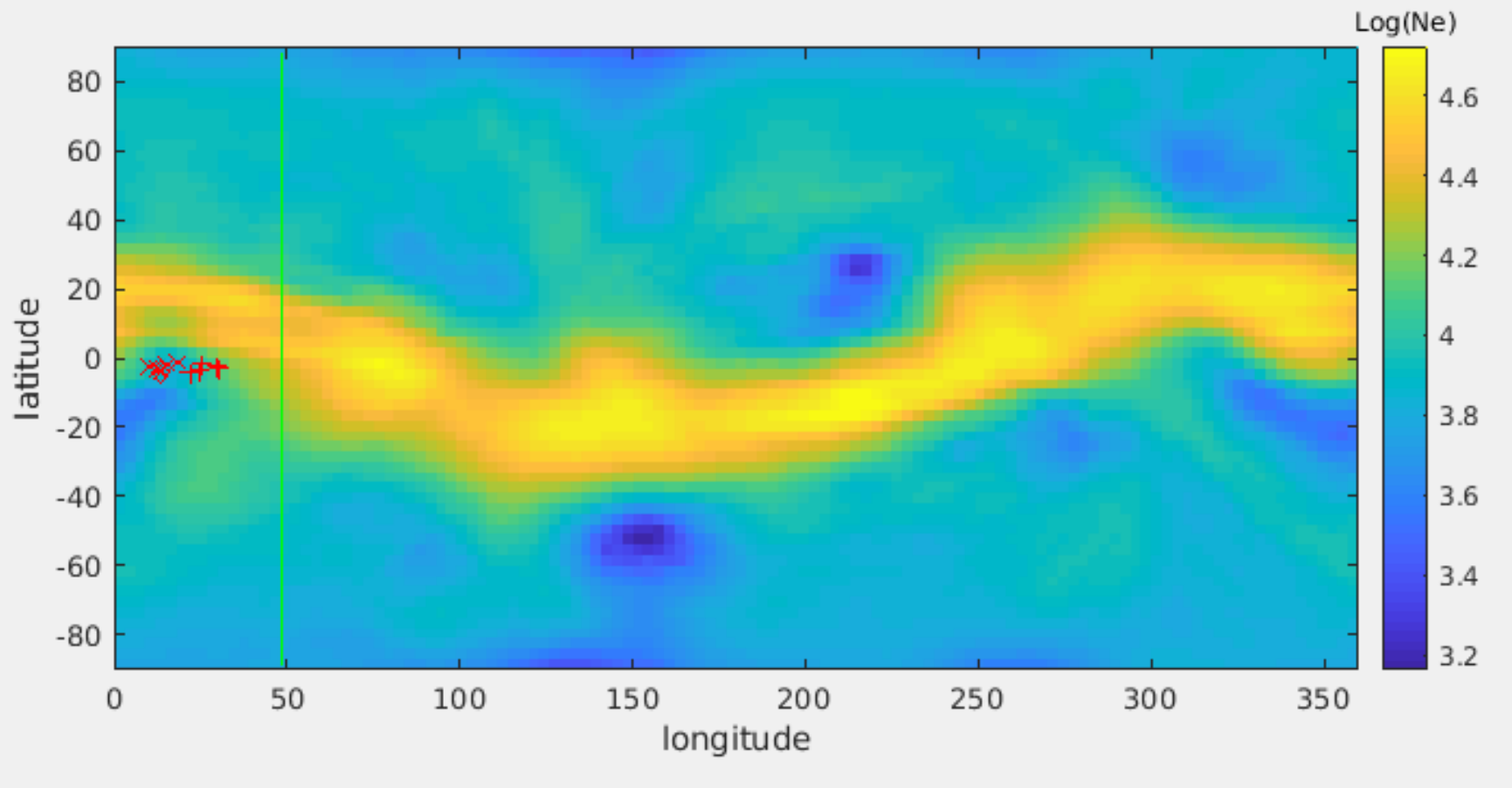
smaller, probably because the Alfvén speed was lower in E2 than E1. The density at perihelion is substantially lower.

Six views of the 3D distribution of the electron density on 2019-04-05 (E2)



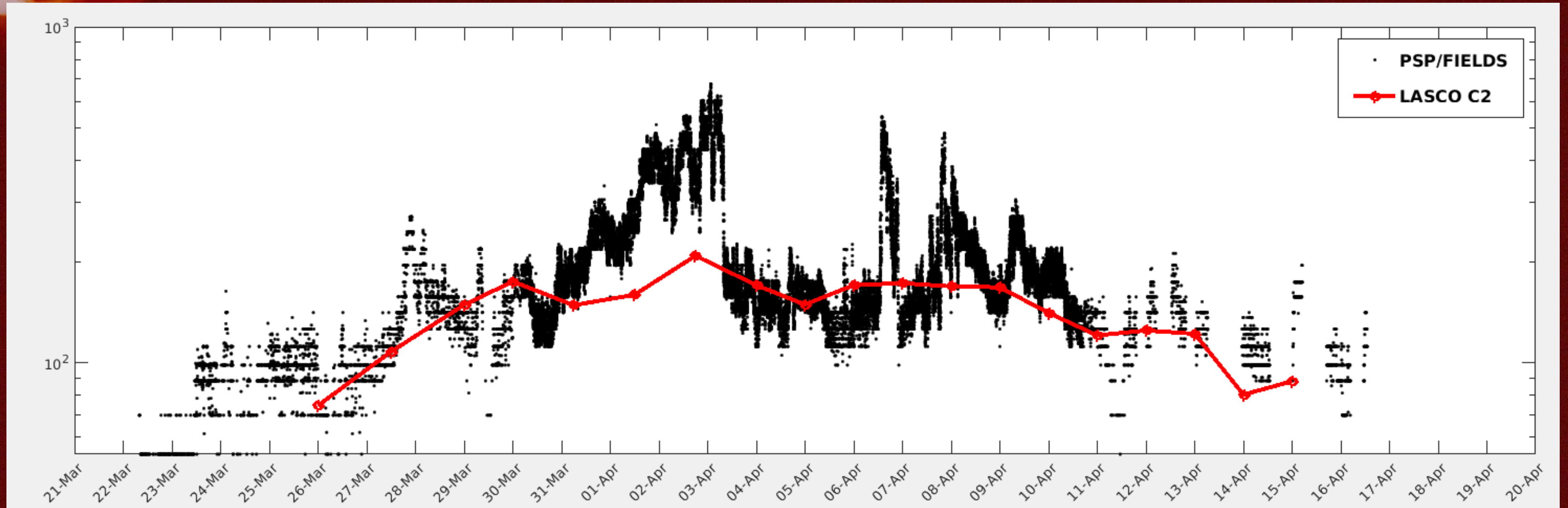
The white sphere has a radius of 2.5 R_{sun}

E2: 2019-03-31 to 2019-04-09



Carrington map and zoomed extract of the electron density (cm^{-3}) at 5.5 R_{sun} and the 11 projected locations of PSP over a time interval of ± 5 days (+) centered at perihelion (\diamond).

Profile of the electron density (cm^{-3}) along the orbit of PSP during E2



Comparison of the profile from PSP/FIELDS measurements (Moncuquet et al. 2019, black line) with the LASCOCO-C2 coronal densities at 5.5 R_{sun} extrapolated to the PSP heliocentric distances using an inverse square law. The time interval of ± 5 days is centered on the perihelion date.

PSP Encounter 4

P4: 2020-01-29 at 0.13AU = 28 R_{sun}

Supporting references:
Chen et al. 2021 ----->
Riley et al. 2021

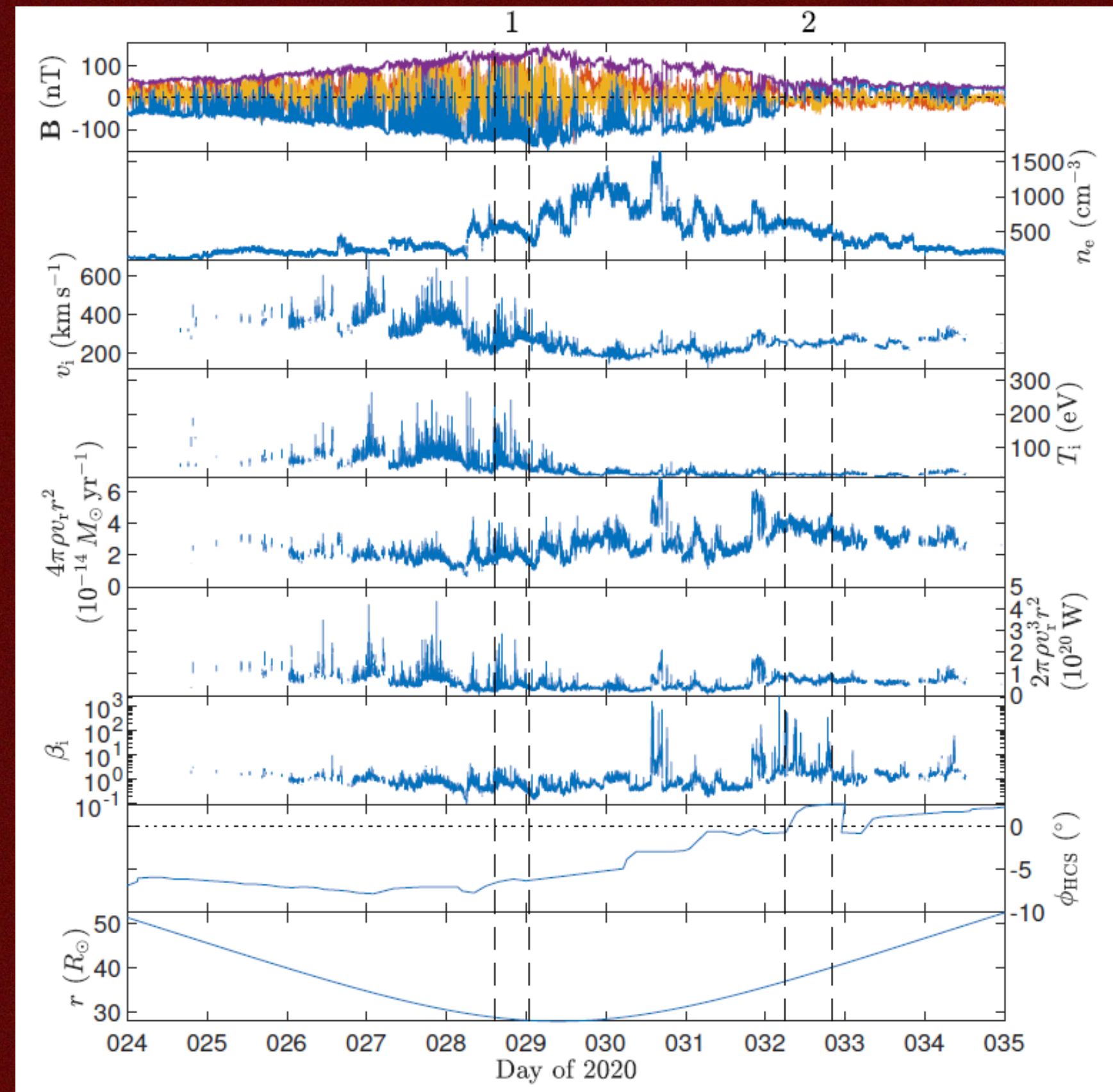
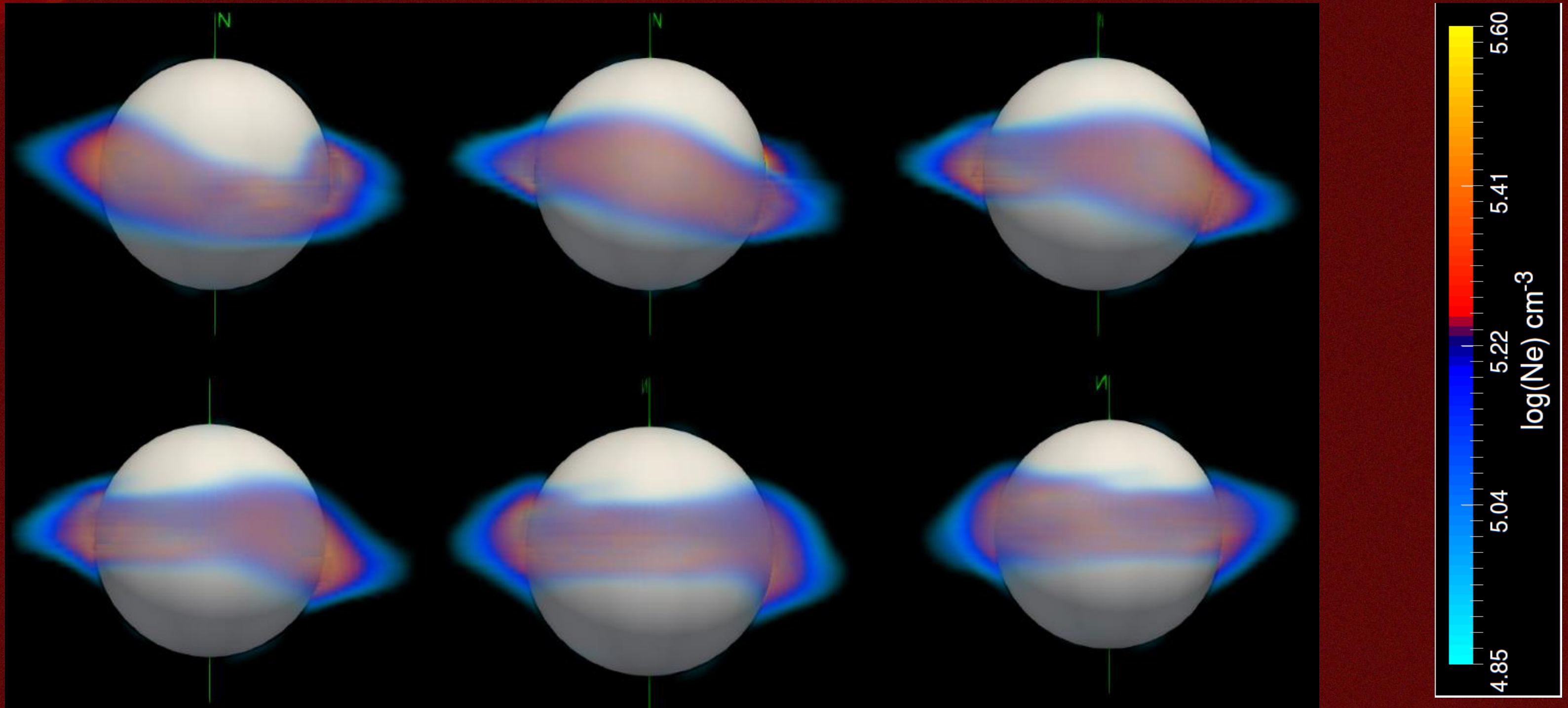


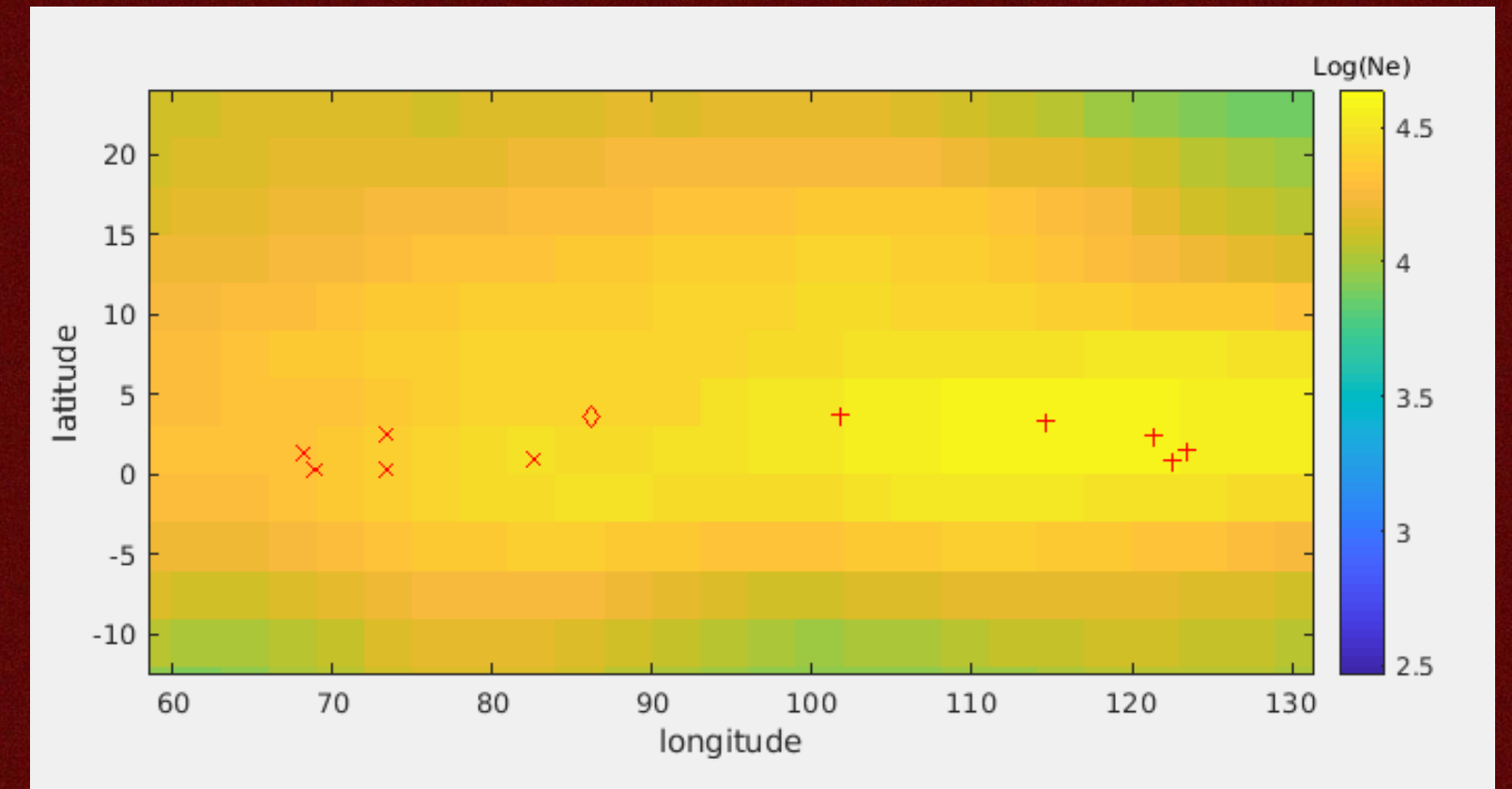
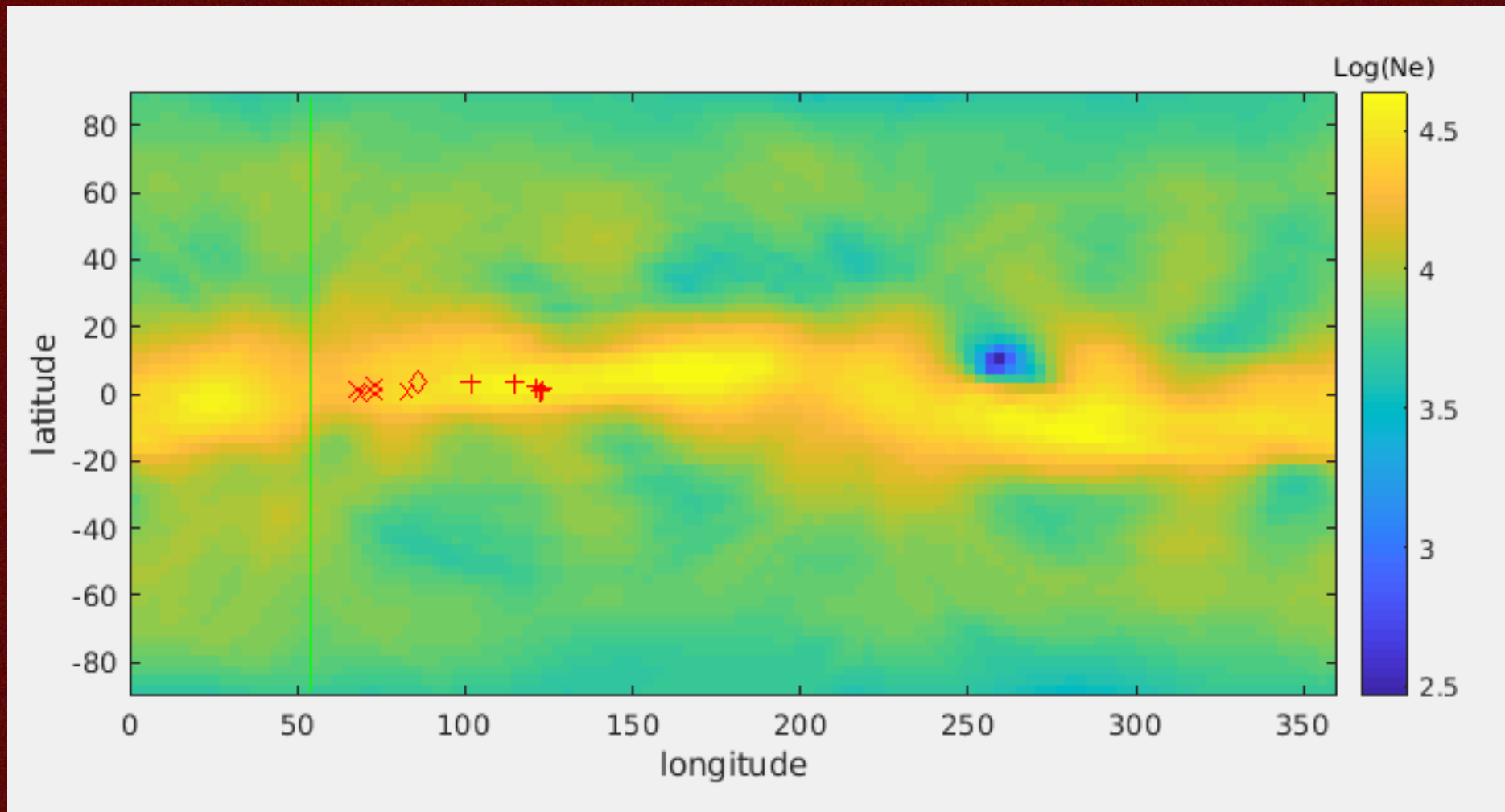
Fig. 1. Time series of Encounter 4 solar wind parameters: Magnetic field \mathbf{B} in RTN coordinates (blue=radial, red=tangential, yellow=normal, purple=magnitude), electron density n_e , solar wind speed v_i , ion temperature T_i , mass flux $4\pi\rho v_r r^2$, energy flux $2\pi\rho v_r^3 r^2$, ion beta β_i , predicted angular distance to the heliospheric current sheet ϕ_{HCS} , and radial distance r . The vertical dashed lines indicate the intervals used to calculate the spectra in Figure 6.

Six views of the 3D distribution of the electron density on 2020-01-29 (E4)



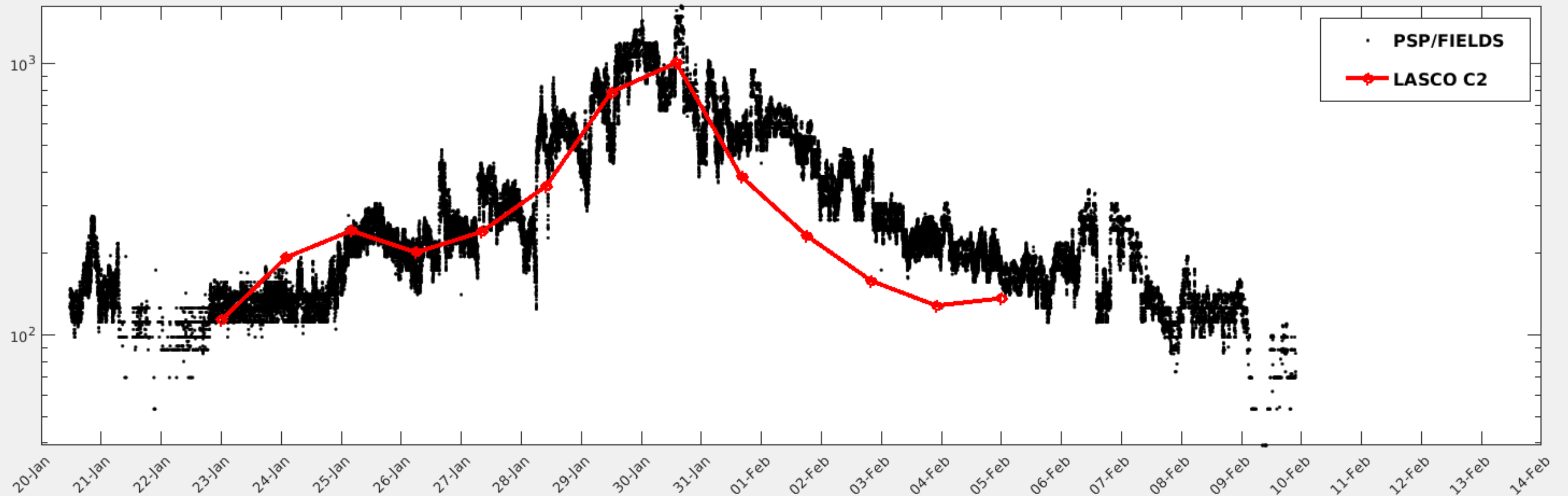
The white sphere has a radius of 2.5 R_{sun}

E4: 2020-01-23 to 2020-02-04



Carrington map and zoomed extract of the electron density (cm^{-3}) at 5.5 R_{sun} and the 11 projected locations of PSP over a time interval of ± 5 days (+) centered at perihelion (\diamond).

Profile of the electron density (cm^{-3}) along the orbit of PSP during E4



Comparison of the profile from PSP/FIELDS measurements (Chen et al. 2021, black line) with the LASCO-C2 coronal densities at 5.5 R_{sun} extrapolated to the PSP heliocentric distances using an inverse square law. The time interval of ± 5 days is centered on the perihelion date.



Discussion

- Bear in mind that we are attempting to connect data from different sources very different acquisition techniques and spatial resolutions.
- Still the agreement is surprisingly good (except for E1)
- These results validate the Ne data from the time-dependent tomographic reconstruction and the inverse square law $N_e \sim 1/R^2$
- The results for E1 are critical dependent on the location of the PSP track with respect to the tiny equatorial hole
- This points to the inherent limitation of applying the ballistic correction and in turn, to using the most appropriate speed of the solar wind
- This limitation will be relaxed as the perihelion distance decreases during the following encounters.



Future work

- Update the tomographic reconstruction at time intervals of 3 to 4 days
- Smooth the solar wind velocity over a TBD time interval
- Extend to other PSP encounters



Thanks to:

- CNES for 25 years of continuous funding
- S. Badman, S. Bale, C. Chen, M. Moncuquet, V. Reville for access to PSP data and many explanations

And thank you for your interest